Mathematical Modelling of the Two Dimensional Flow Behavior of Deformable Rock Fractures

C. Kumara and B. Indraratna
Center for Geomechanics & Railway Engineering, University of Wollongong, Australia

ABSTRACT: Real rock fracture walls are rough surfaces, thus using an average aperture to predict flow through the fractures can produce unrealistic results. Furthermore, flow through rock fractures cannot be considered as unidirectional and therefore it is essential to measure two-dimensional flow behaviour in order to predict fluid flow through underground rock fracture networks. The two dimensional flow equations used in this study were derived by integrating the three dimensional Navier-Stokes equations in the direction of the aperture because it would ensure that the aperture variation in 2D space, which also accommodates aperture deformation against applied confining stress, would be included. The derived equations were discretized by the finite volume method and the numerical solution was proposed by adopting the SIMPLE algorithm. The RFFS (Rock Fracture Flow Solver) computer program was developed using MATLAB to solve the proposed model. RFFS captures the aperture deformations during normal loading, predicts the contact formation accordingly, and also measures the flow patterns and volumetric flow rates. Natural rock specimens with a single fracture were tested on the High Pressure Two Phase Triaxial Apparatus (HPTPTA) designed and built at the University of Wollongong, while the measured flow rates and RFFS predictions for different confining stresses and hydraulic gradients were compared and found to be in acceptable agreement; the directional permeabilities were calculated by RFFS predictions.

1 INTRODUCTION

The permeability of jointed rock is a significant factor for industrial activities such as underground excavations and nuclear waste repositories, and the permeability of single rock fracture is usually measured using the cubic formula given in Eq. 1 (Lomize 1951; Snow 1968; Witherspoon et al. 1980).

$$Q = \frac{e^3 w}{12\mu}\nabla P \qquad (1)$$

where Q is the flow rate, e is the aperture, μ is the dynamic viscosity of the fluid, w is the width of the fracture under consideration and ∇P is the hydraulic gradient. Fracture aperture is spatially not constant because of its irregular nature, and an average or equivalent aperture should be considered to use the cubic formula which may overestimate the volumetric flow rates (Barton et al. 1985; Neuzil and Tracy 1981; Zimmerman et al. 1992; Zimmerman et al. 2004).

To overcome this problem, different methods of calculating the equivalent permeability have been suggested, and two dimensional models have also been proposed. There are two types of 2D models, both based on the physical model, where the first considers the height of the aperture and direction of flow as two dimensions (Indraratna et al. 2002; Koyama 2007; Price and Indraratna, 2005), while the second assumes the direction of flow and the width of the fracture as the two dimensions for formulating the model (Bear et al., 1993; Kishida et al. 2013). The latter method was used in this study because the two-dimensional flow behaviour can be studied and the deformation and contact formation of the fracture that affects flow behaviour can be modelled.

2 MATHEMATICAL MODEL

Eq. 2 is the 3D Navier-Stokes equation for a homogeneous and Newtonian incompressible fluid (Bear et al. 1993).

$$\frac{\partial(\rho\bar{V})}{\partial t} + \nabla\cdot(\rho\bar{V}\bar{V}) + \nabla p - \rho g\nabla Z - \mu\nabla^2\bar{V} = 0 \qquad (2)$$

where ρ is the fluid density, $\bar{V}$ is the fluid velocity vector, p is the fluid pressure, g is the gravitational acceleration and Z is the direction of gravity. Eq. 2 was integrated in the direction of the fracture aperture by taking the fracture walls as the limits of integration (Indraratna et al. 2014). Here, the limits were also functions of time and space; the resulting momentum conservation is given in Eq. 3, while the ‘dot’ over the velocity and divergence operator indicates they were only applied in the remaining two dimensions after integration. Here $e(x, y, t)$ is the aperture.

$$\frac{\partial\left(\rho e\bar{\dot{V}}\right)}{\partial t}+\dot{\nabla}\cdot\left(e\rho\bar{\dot{V}}\bar{\dot{V}}\right)+e\dot{\nabla}p-\rho g e\dot{\nabla}Z-\mu\dot{\nabla}^{2}\left(e\bar{\dot{V}}\right)+\frac{12\mu}{e}\bar{\dot{V}}=0 \quad (3)$$

The continuity equation was then integrated in the same way, and the following 2D continuity equation was obtained.

$$\dot{\nabla}\cdot\left(\rho e\bar{\dot{V}}\right)=0 \quad (4)$$

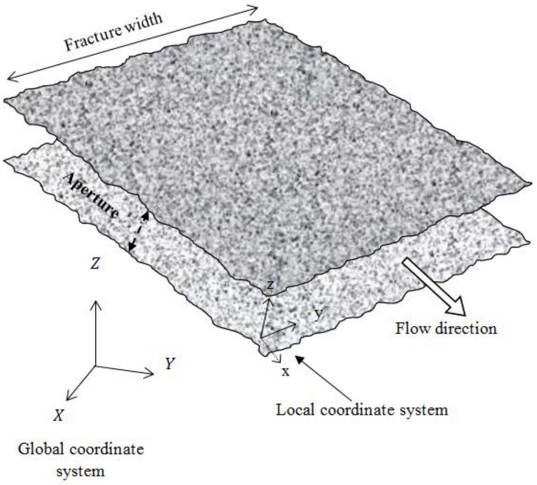

Fig. 1 Single rock fracture model

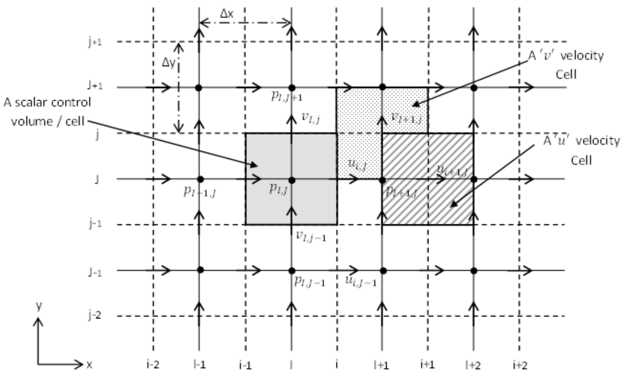

Fig. 2 Discretization of flow domain using FVM (Indraratna et al., 2014).

Fig. 1 shows the physical model of a single rock fracture considered in the mathematical model, showing the direction of flow and dimensions of the fracture. Eqs. 3 and 4 are the governing equations for the model and for the steady flow conditions, the temporal acceleration term of Eq. 3 can be omitted. The model had to be solved numerically due to the non-linearity of the equations, so the finite volume method was used to discretize (Fig. 2) the equations in their scalar form.

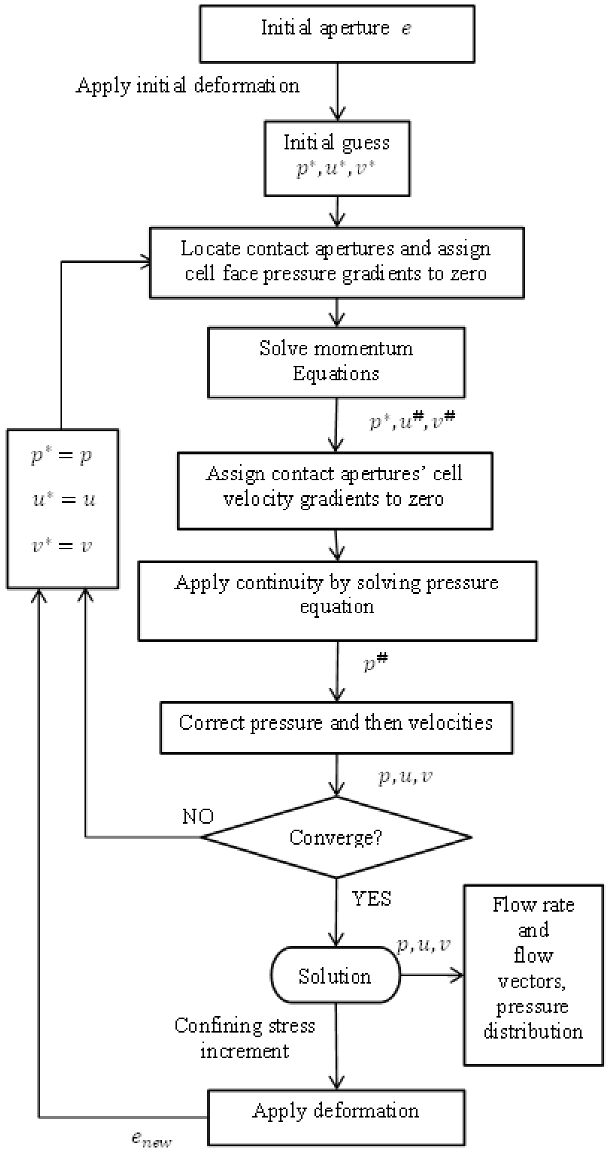

Fig. 3 Flow chart for modified SIMPLE algorithm (Indraratna et al. 2014)

SIMPLE (Semi Implicit Method for Pressure Linked Equations) algorithm (Patanker and Spalding, 1972) was modified and used to develop the numerical solution. A new computer program called the Rock Fracture Flow Solver (RFFS) was developed using MATLAB language to execute the numerical solution (Indraratna et al., 2014; Kumara, 2014).

3 METHODOLOGY & FLOW SIMULATION

The Rock Fracture Flow Solver followed the flow chart in Fig. 3 and solved the discretized governing equations to calculate the distribution of pressure and velocity. The rock fracture deformations were calculated using the hyperbolic relationship suggested by Bandis et al. (1983). After deformation the contact formation was captured by a special algorithm. When the aperture of a certain control volume of the flow domain becomes smaller than a threshold limit for a contact, the particular control volume is flagged as a contact to consider in the following iterations.

Sandstone specimens 54mm in diameter were split in the laboratory and single axial fracture samples were prepared. By shifting the two halves in opposite direction, mismatched specimens were created. The aperture distribution was measured by injecting a fast setting epoxy resin into the fracture. Once set, one half of the specimen was removed and the silicon rubber surface or the replica of the removed rock fracture surface was scanned using a 3D laser scanner. Next, the surface of the remaining half was scanned with respect to the same origin such that the difference between the two surfaces resulted in the fracture aperture distribution (Fig. 4). The aperture distribution, fluid inlet and outlet pressures, specimen dimensions, normal loading, and the properties of the fluid (density, viscosity) and the fracture (initial fracture normal stiffness) were fed into the RFFS, which then produced a 2D flow simulation with aperture distribution and pressure distribution at applied normal loading conditions in order to compare the flow rate and deformation changes against normal loading. The rock fracture permeability was tested in the laboratory using the High Pressure Two Phase Triaxial Apparatus (Indraratna and Haque 1999), and the flow rates for increasing confining pressures were obtained.

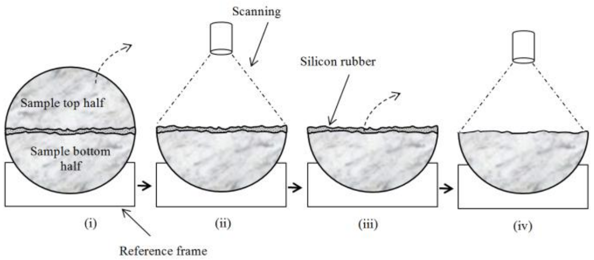

Fig. 4 Aperture distribution measurement (Indraratna et al. 2014)

4 RESULTS & DISCUSSION

Fig. 5 shows the normal deformation of a rock fracture upon loading, via the contours of the aperture, with flow vectors for a mismatched fracture specimen. The white patches are the contacts that were captured by RFFS according to the fracture closure data; this model also showed the two-dimensional flow behavior inside the fracture more realistically. The fluid flowed through the fractures and avoided the obstacles (contacts and smaller apertures), and therefore the permeability of the same fracture in two orthogonal directions was not the same. RFFS can be used to measure the permeability through a rock fracture in both major directions, whereas the mated joints showed less diverging flows because the range of aperture variations was narrow.

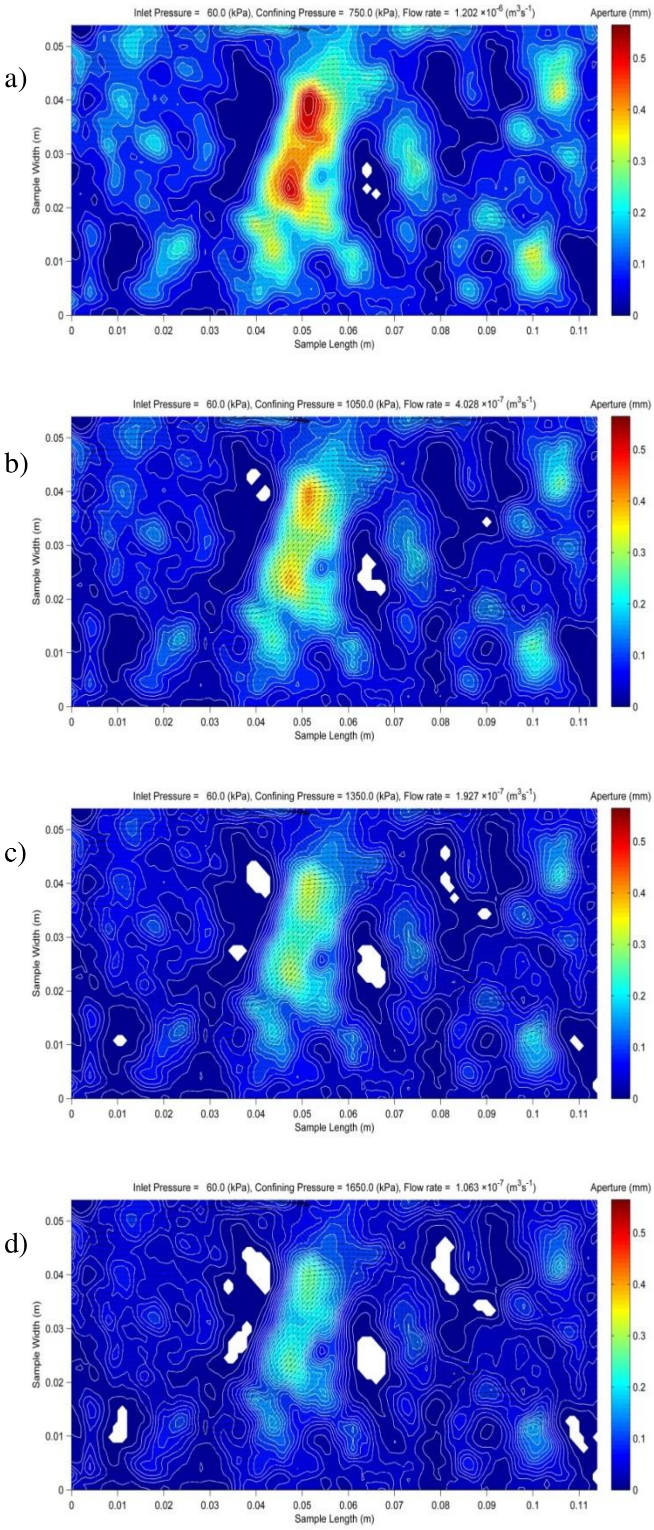

Fig. 5 Aperture deformation (contours) and flow patterns (arrows) of a single rock fracture at confining stresses (a) 750 kPa (b) 1050 kPa (c) 1350 kPa (d) 1650 kPa.

The accuracy of the RFFS predictions for the longitudinal direction (Indraratna et al. 2014), was verified elsewhere. Having changed the boundary conditions of the flow domain, the flow and deformation data for the rock fractures were obtained in a transverse direction. Directional permeabilities were calculated considering the macroscopic flow domain according to the Darcy's formula for different normal stresses. Fig. 6 shows the variations in permeability against the normal stress applied for longitudinal and transverse directions for the same specimen, illustrated in Fig. 5. Since the openings elongated in the transverse direction was larger than the surrounding aperture of the domain, permeability in that direction has risen more than in the longitudinal direction.

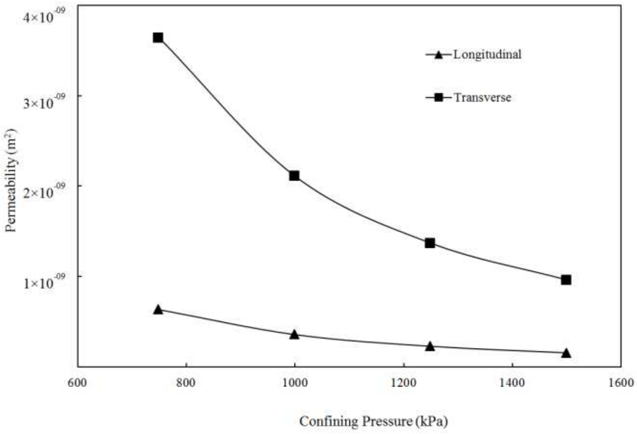

Fig. 6 Variation in the Longitudinal and Transverse directional permeability of a mismatched specimen against normal loading

5 CONCLUSIONS

A 2D mathematical model with a solution program was proposed to simulate two dimensional single fracture flows. This model was then used to calculate the flow volumes and patterns in the flow domain, and capture the contact formation upon normal loading realistically. The directional permeability of rock fractures was computed using this developed computer programme, and their dependence on the aperture distribution was demonstrated. The longitudinal directional permeability of the specimen was $6.35\times10^{-10}m^2$ while the transverse directional permeability was 3.64×10^{-09} at 750 kPa confining stress; this result was due to the flow domain having the larger apertures elongated in a transverse direction. When the confining stress was gradually increased to 1500 kPa, the differences between the directional permeabilities decreased because larger apertures deform much more than smaller apertures. The mated joints had negligible differences in directional permeabilities because their aperture distribution was not scattered widely. It can be concluded that fracture permeability differs along the flow directions depending on the directional distribution of the larger apertures of the flow domain.

ACKNOWLEDGEMENTS

The authors acknowledge the ARC linkage project for funding and the University of Wollongong technical staff for assisting with laboratory experiments.

REFERENCES

Barton, N., Bandis, S., and Bakhtar, K., (1985)., Strength, Deformation and Conductivity Coupling of Rock Joints, Int. J. Rock Mech. Min. Sci. 22(3): 121-140.

Bear, J., Tsang, C. F., de Marsily, G., (1993)., Flow and contaminant transport in fractured rock, Academic Press, California.

Indraratna, B., and Haque, A., (1999)., Triaxial equipment for measuring the permeability and strength of intact and fractured rocks, Geotechnique, 49(4): 515-521.

Indraratna, B., Price, J., and Gale, J. 2002 Fourier description of fracture roughness, 5th North American Rock Mechs Symp., University of Torronto Press, Torronto, pp 35-44.

Indraratna, B., Kumara, C., Zhu, S., Sloan, S., (2014)., Mathematical Modeling and Experimental Verification of Fluid Flow through Deformable Rough Rock Joints, International Journal of Geomechanics, DOI:10.1061/(ASCE)GM.1943-5622.0000413.

Kishida, K., Sawada, A., Yasuhara, H., and Hosoda, T., (2013)., Estimation of fracture flow considering the inhomogeneous structure of single rock fractures, Soils and Foundations, 53(1): 105-116.

Koyama, T. (2007). "Stress, Flow and Particle Transport in Rock Fractures" PhD thesis, Department of Land and Water Resources Engineering, Royal Institute of Technology (KTH), Stockholm.

Kumara, C. (2014). "Load-deformation behaviour of rough rock fractures subjected to internal water flow" PhD thesis, School of Civil, Mining, and Environmental Engineering, University of Wollongong, Wollongong.

Lomize, G. M. (1951), Flow in Fractured Rocks (English Translation), Gosenergoizdat, State Press

Neuzil, C. E., and Tracy, J. V., (1981)., Flow through fractures, Water Resour. Res., 17(1): 191-199.

Patanker, S. V., Spalding, D. B., (1972)., A calculation procedure for heat, mass and momentum transfer in three-dimensional parabolic flows, Journal of Heat and Mass Transfer, 15(10): 1787-1806.

Price, J., and Indraratna, B., (2005)., Development of an equivalent homogenous fluid model for pseudo-two-phase (air + water) flow through fractured rock, J. Geotech. Geoenviron. Eng., 131(7): 857-866.

Snow, D. T., (1968)., Rock fracture spacings, openingsand porosities, Soil Mech. Found. Div., ASCE **94(SMI)**: 73-91.

Witherspoon, P. A., Wang, J. S. Y., Iwai, K., Gale, J. E., (1980), Validity of Cubic Law for Fluid Flow in a Deformable Rock Fracture, Water Resource Res., **16**(6): 1016-1024.

Zimmerman, R. W., Chen, D.W., Cook, N. G. W., (1992)., The effect of contact area on the permeability of fractures, Journal of Hydrology, 139(1–4): 79-96.

Zimmerman, R. W., Al-Yaarubi, A., Pain, C. C., Grattoni, C. A., (2004)., Non-linear regimes of fluid flow in rock fractures, Int. J. Rock Mech. Min. Sci., 41: 163-169.